12

INTRODUCTION TO NMR AND ITS APPLICATION IN METABOLITE STRUCTURE DETERMINATION

Xiaohua Huang, Robert Powers, Adrienne Tymiak, Robert Espina, and Vikram Roongta

12.1 INTRODUCTION

The broad utility of nuclear magnetic resonance (NMR) was first recognized in 1951 from a series of experiments that observed a relationship between chemical structure and corresponding shifts in the NMR resonances. Since that time, NMR has evolved from continuous wave (CW) spectroscopy to Fourier transform (FT) spectroscopy, from permanent magnets to super conducting magnets and from one dimensional to multidimensional NMR spectra. The range of NMR applications has also grown significantly and includes (i) chemical structure elucidation (Breitmaier, 2002; Martin and Zektzer, 1988) (ii) three-dimensional conformational studies of biomolecules (Betz, 2006; Pellecchia, 2005), (iii) analysis of enzyme kinetics (Schutz et al., 2005), (iv) determination of reaction mechanisms (Lyčka et al., 2007; Moreno et al., 1996; Munro and Craik, 1994; Schaefer 1982), and (v) ligand binding screening for drug discovery (Hajduk, 2006; Lepre et al., 2004; Orry et al., 2006; Zartler et al. 2006). In the field of drug metabolism (Corcoran and Spraul, 2003), NMR is an extremely valuable tool in understanding biotransformation pathways and the potential involvement of metabolites in observed drug toxicities. Metabolite structure elucidation is particularly useful when the site of metabolism cannot be readily assigned by other techniques.

Drug Metabolism in Drug Design and Development, Edited by Donglu Zhang, Mingshe Zhu and W. Griffith Humphreys

In this chapter we provide a brief introduction to NMR theory and describe the most common experiments used for metabolite structure determination by NMR. Selected examples of metabolite structure elucidation are presented to illustrate relevant hardware, key parameters, and NMR methodology. Detailed explanations of NMR fundamentals have been previously reviewed in a series of books that are listed at the end of this chapter (Berger and Brunn, 2004; Breitmaier, 2002; Freeman, 1997; Friebolin, 2005; Homans, 2005; Keeler, 2005; Martin and Zektzer, 1988).

12.2 THEORY

An NMR signal arises from an interaction between the nuclear spin (I) of an atom with an external magnetic field (B_0). Elements with even atomic mass and number have a zero nuclear spin, where only nuclei with $I \neq 0$ produce an observable NMR signal. Nuclei with $I > ½$ generate broad resonance lines in an NMR spectrum and are not generally useful for structure elucidation. Fortunately, most of the elements that comprise metabolites correspond to nuclei that are observable by NMR. They are listed in Table 12.1 along with their relevant NMR properties.

The intensity of the NMR signal depends on both the strength of the magnetic field (B_0) and the magnitude of the magnetogyric ratio (γ), an intrinsic physical property for each nucleus. Of the elements listed in Table 12.1, ^{3}H is the most sensitive nucleus but has limited application due to its low natural abundance and radioactivity. ^{1}H has the second highest sensitivity, has 100% natural abundance, is prevalent in the majority of organic and bioorganic molecules, and correspondingly, is the most frequently detected nucleus for structure characterization of organic molecules, ^{13}C, ^{15}N, ^{31}P, and ^{19}F NMR spectra are also commonly collected as part of a structure determination project.

TABLE 12.1 NMR Properties for common nuclei.

Nuclide	Spin I	Natural abundance (%)	Gyromagnetic ratio gamma (10^7 rad T^{-1} s^{-1})	NMR frequency (MHz) (B_0 = 14.09 T)
^{3}H	1/2	—	28.535	639.978
^{1}H	1/2	99.98	26.7519	600.000
^{2}H	1	0.016	4.1066	92.106
^{13}C	1/2	1.108	6.7283	150.864
^{15}N	1/2	0.37	−2.712	60.798
^{19}F	1/2	100	25.181	564.462
^{31}P	1/2	100	10.841	242.886
^{10}B	3	19.58	2.8746	64.476
^{11}B	3/2	80.42	8.5843	192.504

The intensity of the NMR signal is extremely small when compared to all other types of spectroscopy due to the small energy gap between nuclear spin states (α, β). For a given nucleus, the increase in sensitivity is directly proportional to the magnetic field produced by the magnet; therefore, greater sensitivity is achieved as the magnetic field strength is increased.

When a chemical sample is placed within this magnetic field, the nuclear spins either align with the external magnetic field (α) or align against it (β), The α spin state is at a lower energy and is more populated than the β spin state under equilibrium conditions. In a classical description of spinning particles in a magnetic field, a net magnetization created by an ensemble of spins is depicted as a vector along the *Z*-axis (Fig. 12.1). The NMR signal results from perturbing this equilibrium and inducing a spin transition from the α to β state by applying a radio frequency pulse (rf) perpendicular to the *Z*- axis. The frequency of the rf pulse must be proportional to the energy gap separating the α and β spin states. Since an rf pulse also contains a magnetic vector, the process can also be viewed as the net magnetization precessing about the new B_1 field created by the rf pulse (Fig. 12.2). The duration and direction of the rf pulse determines the orientation of the net magnetization vector when the rf pulse is terminated. A 90° pulse is typically applied and results in the net magnetization along the *Z*-axis being "flipped" into the *X*,*Y* plane.

After the rf pulse, the net magnetization will continue to precess in the *X*,*Y* plane about the external magnetic field (B_0). The system will also slowly relax back to the *Z*-axis equilibrium position. The frequency of the *X*,*Y* precession, also known as the Larmor frequency, is related to B_0, γ, and more importantly, to the local chemical environment of the nucleus. Small differences in the chemical environment of a nucleus will result in parts per million (ppm) differences in the Larmor frequency, which is known as the NMR Chemical

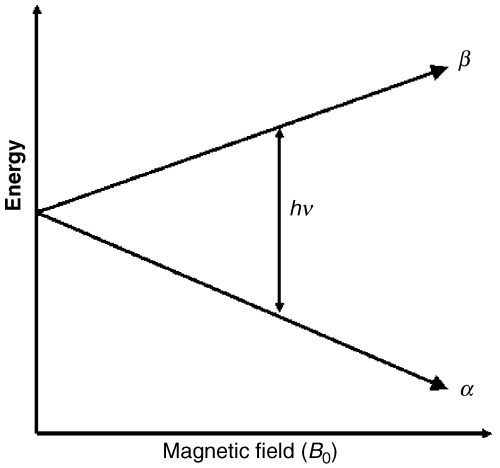

FIGURE 12.1 Relationship between the magnetic field strength and NMR sensitivity.

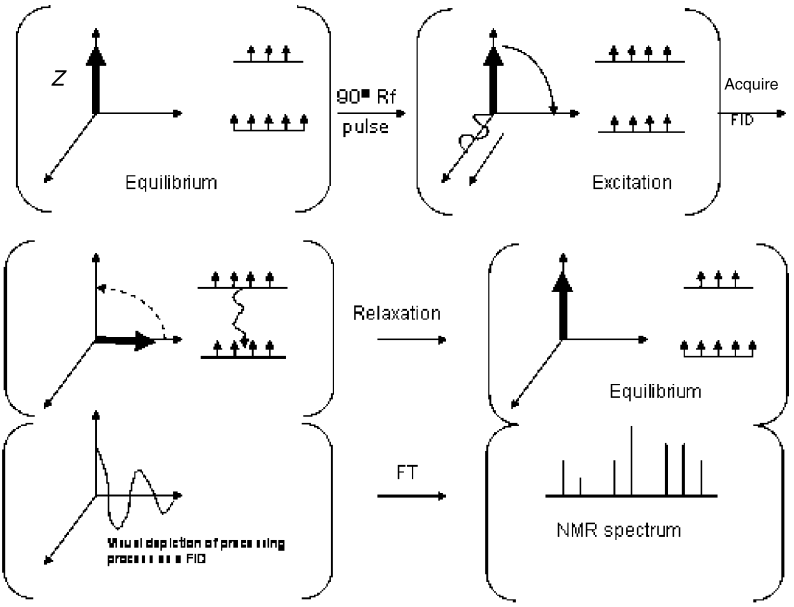

FIGURE 12.2 Scheme of one pulse, one-dimensional NMR experiment.

shift. This precessing process is captured as a free induction decay (FID) by monitoring the variation in an induced current in receiver coils positioned perpendicular to the *X*-,*Y*- axis. The FID is typically monitored for duration of milliseconds to seconds. This basic NMR process is called a one pulse, one-dimensional (1D) experiment.

A high power, short duration (hard) rf pulse will simultaneously perturb all the ^{1}H, ^{13}C, or ^{15}N nuclei in a molecule creating a FID that includes the NMR resonances of all these nuclei. The observed FID is a complex combination of sine and cosine wave oscillations at multiple frequencies in the time domain. The FID is transformed to a conventional frequency-domain NMR spectrum by applying a FT as depicted in Fig. 12.2.

12.3 NMR HARDWARE

The major components of an NMR spectrometer include a with a magnet, probe, rf electronics, and a desktop computer as depicted in Fig. 12.3 and further described in Table 12.2. Significant advancements in NMR hardware over the years have yielded dramatic increases in experimental sensitivity and resolution. One such advancement has been the recent introduction of the shielded 900 MHz magnet. A 900 MHz magnet results in an 84% improvement in sensitivity and a 150% improvement in resolution relative to a standard 600 MHz magnet (Kupce, 2001). The shielded aspect of the magnet reduces the

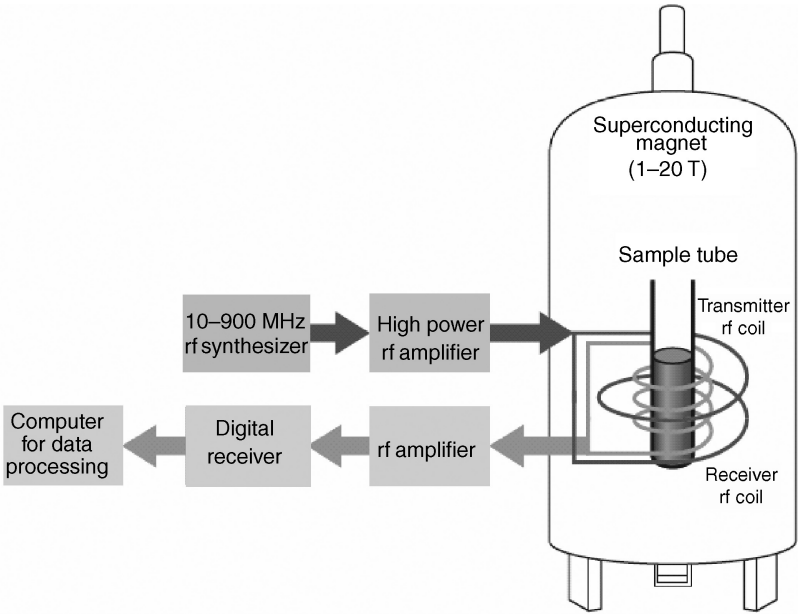

FIGURE 12.3 Scheme of a NMR system and its components.

5-gauss line by one-fourth, which needs to be shielded from personnel and other equipment, resulting in a significant reduction in laboratory space and cost. Another major advancement has been the introduction of cryoprobes (Bruker Biospin, 2002; Varian Inc, 2002), (Bieri et al., 2006; Keun et al., 2002) that has resulted in a three to five fold increase in sensitivity by reducing electronic noise by cooling the receiver electronics to near liquid helium temperature.

12.4 NMR OBSERVABLES

An NMR spectrum contains four important experimental observables, chemical shifts, coupling constants, peak intensity (integration), and peak width (relaxation time), that provide quantitative measurements of the structure, dynamics, and nuclei count of the chemical entity being studied. Chemical shifts and coupling constants provide direct evidence for identifying what functional groups are present in the structure and for assigning bond connectivity and spatial relationships between atoms (stereochemistry). Intensities of the NMR peak provide a relative measure of the quantity or count of the specific nuclei in the sample. The peak width is proportional to the T_2 relaxation time, which is related to dynamic processes such as chemical exchange or reaction kinetics. A second relaxation time (T_1) is related to the net magnetization relaxing back to its equilibrium position after an rf pulse. A summary of these basic NMR characteristics is tabulated in Table 12.3.

TABLE 12.2 Common NMR hardware and its new developments.

	Conventional design	New developments	Advantages
Magnet	Super conducting magnet.	Shielded and ultra shielded magnet. The extra outer magnet coil cancels the stray field from the inner coil of the magnet to reduce the 5-gauss line significantly	Field strength could go up to 900 MHz. High stability and homogeneity. Shielded magnets need much smaller space to site a magnet It is easy to couple the NMR spectrometer with mass spectrometer or HPLC systems.
Probe	5 mm or 3 mm CH dual probe, QNP probe, TXI probe, Broadband probe.	Cryocooled probe in which the probe rf coil and the preamplifier are close to liquid helium temperature	The sensitivity of ^{1}H and ^{13}C is three to four times higher than that of a conventional probe. Significant reduction in time for 2D NMR experiments1D ^{1}H can be obtained with as little as 10 ng of compound
		Capillarycoil probe that with a receiver coil that is 10–100 times smaller than that of the conventional probe.	High mass sensitivity Less sample and solvent consumption
		Flow (tubeless) probe that use direct injection (manual or automatic) to deliver sample to the flow cell.	Can be directly coupled with HPLC and MS spectrometer (NMR–HPLC–MS). Is used for 96- or 384-plate analysis in a high throughput mode.
Console and computer	It consists of robust components: frequency generator, radio frequency and gradient amplifiers, interface board, shimming board and signal generator and detector.	Digital-signal processor.Faster computer.Noise free and linear amplifiers. Gradient shimming.	Increases linearity of excitation over wider range of excitation Improvements in baselineReduced processing time for large data sets

TABLE 12.3 Properties of common NMR spectral characteristics.

Chemical shifts	Coupling constants	Integration	Relaxation times
Chemical shift of a nucleus depends on its electronic environment and the magnitude of the local magnetic field	Interaction of nonequivalent atoms through bonds, generally 1-, 2- and 3-bonds distances.	Integration of a ^{1}H spectrum provides quantitative information	Nuclei return to the equilibrium state after excitation by various mechanisms. Two most common ones are described below
$B_{eff} = B_0 - \sigma B_0$ B_0 = main field B_{eff} = reduced field $nu = \gamma/2\pi\ (1 - \sigma)B_0$	Coupling patterns or multiplicity: $M = 2nI + 1$ M = Multiplicity n = number of equivalent nuclei I = ½ for most of the nuclei	In ^{1}H spectra, integral of each peak determines the number of hydrogens present in the structure	T_1 relaxation Spin–Spin relaxation
		The equivalent Hydrogens on a methyl, CH_3 residue integrate to three times the area compared to a methine CH residue	Determines the interaction of spins that are close to each other T_1 relaxation time depends on the other spins in the molecule
Chemical shift scale is a parts per million (ppm) scale. The ^{1}H and ^{13}C scale is referenced to 4-trimethyl silane (TMS) at 0 ppm	Common homo-nuclear coupling $^{1}H-^{1}H$ and $^{19}F-^{19}F$	External compound of known amount is used to quantitate the amount of compound in the solution	T_1 is extremely critical for optimizing all the NMR experiments

(*continued*)

TABLE 12.3 (*Continued*)

Chemical shifts	Coupling constants	Integration	Relaxation times
$> \delta = (\nu_{sample} - \nu_{ref})/\nu_{ref} \times 10^6$ For a spectrometer $\delta = \Delta\nu$/spectrometer frequency $\times 10^6$	Heter-nuclear coupling $^1H-^{13}C$, $^1H-^{15}N$, $^1H-^{19}F$, $^{13}C^{19}F$ Magnitude of coupling constants	Integration is often used to quantitate impurities or estimate the percentage of residual solvents Integral is not commonly measured for carbons	T_2 relaxation Spin–lattice relaxation T_2 relaxation times depend on the media of the molecule.
The scale goes from 0 ppm on left to higher ppm on the right ^1H range 0 ppm to 20 ppm ^{13}C range 0 ppm to 220 ppm	$^1H-^1H$, 1, 2, and 3 bonds ~1 Hz to 20 Hz $^1H-^{13}C$ bond ~140 Hz $^1H-^{15}N$ bond ~90 Hz		
The chemical shift value of a residue in a particular molecule does not change at different field strengths	The magnitude of a coupling-constant between two residues in a particular molecule does not change with field strength	Ratio of integral values between residues in a particular molecule does not change with field strength	Solvent, viscosity, temperature affects the line width. Short T_2 value results in broader peaks and Long T_2 results in narrower peaks

12.4.1 Chemical Shifts

The electronic environment of a nucleus is determined by the spatial arrangement of adjacent atoms and electrons. This local environment influences the effective magnetic field experienced by the nucleus. Typically, a nucleus is shielded, to a certain extent, from the external magnetic field (B_0) by its local environment and experiences only a fraction of the strength of B_0 and correspondingly exhibits a lower Larmor frequency. The result is a distinct chemical shift for each nucleus present in the molecule that exists in a unique local environment. The observed chemical shifts are characteristics of these environments and are very sensitive to subtle changes, where a ^{1}H in an aromatic ring differs from a ^{1}H attached to an electrophile (O, N, etc.). Among the NMR active nuclei, chemical shifts of the ^{1}H nuclei in a molecule are the most sensitive to the changes in solvent, pH, ionization state, temperature, and aggregation state of the molecule. Examples of ^{1}H and ^{13}C chemical shift ranges for different functional groups are listed in Table 12.4.

12.4.2 Coupling Constants

Chemically nonequivalent nuclei in a molecule can couple with each other through bonds, where the magnitude of this interaction (Hz) is smaller than a chemical shift (ppm) and is described by a coupling constant (J). The coupling of spins causes a mixing of the α and β spin states associated with each nucleus in the coupled system. The result is a multiplet ($n + 1$) peak pattern where the number of peaks for each coupled spin is determined by the number of nuclei (n) coupled to it. The separation between the peaks in the multiplet corresponds to J and the relative intensities of the peaks follows Pascal's triangle. The strength of this through bond coupling interaction decreases proportionally with the number of intervening bonds, and is generally observable for coupling between one, two, and three bonds, but has been observed for nuclei separated by as many as nine bonds. NMR coupling can be

TABLE 12.4 Typical ^{1}H and ^{13}C chemical shift ranges for organic functional groups.

Residues	^{1}H (ppm)	^{13}C (ppm)
R−CH_3, R−CH_2, RCH, R=C, S,	0.5–3.5	10–30
R−CH_3, R−CH_2, RCH, R=N	2.5–4.5	35–55
R−CH_3, R−CH_2, RCH, R=O	3.5–5.5	60–75
Vinyl HRC=CHR	5–7	100–150
Aromatic	6–9	110–160
Amide NH hydrogens	7–15	
Carbonyls carbons		155–220
Aldehydes	9–10	180–200

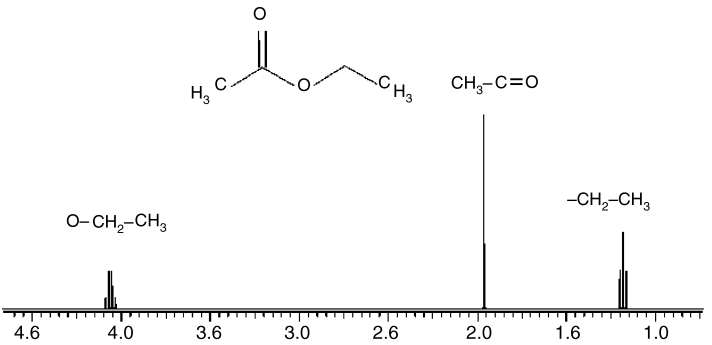

FIGURE 12.4 Simulated ^{1}H NMR spectrum of ethyl acetate.

illustrated with a simulated stick spectrum as demonstrated for ethyl acetate in Fig. 12.4.

The methyl signal (lowest chemical shift) is split into a triplet because of coupling to the two adjacent hydrogens of the methylene group, and the methylene is split into a quartet because of coupling to the three hydrogens of the adjacent methyl group. The methyl group next to the carbonyl group appears as a singlet since it is isolated from through bond interactions with the other hydrogens.

^{1}H$-^1$H coupling constants are commonly used for structure elucidation to help identify which NMR resonances (functional groups) are chemically bonded as evidenced by observation of a shared coupling constant. Using the ethyl acetate example in Fig. 12.4, the observation that the peak separation between the methyl triplet and methylene quartet are equivalent (same J) indicates that these two functional groups must be chemical bonded in the ethyl acetate structure. The magnitude of the ^{1}H coupling constant also reflects the electronic environment, bond angle between the hydrogens involved, bond distance, and the hybridization state of the carbon to which the hydrogen atoms are attached. Some of the common ^{1}H$-^1$H coupling constants are listed in Table 12.5.

TABLE 12.5 Common ^{1}H$-^1$H coupling constants.

Alkane vicinal	Geminal	Double bonds
(^{1}H)R2C$-$CR2(^{1}H)	RC(^{1}H)(^{1}H)	Geometry
Gauche: $^3J \sim 5$ Hz	$^2J \sim 0 - 30$ Hz	$^3J_{trans} = 12 - 18$ Hz
Trans: $^3J \sim 10$ Hz		$^3J_{cis} = 6 - 12$ Hz
Aromatic protons	Cyclo hexane type rings	Small rings cyclo propane, butane and pentane
$^3J_{ortho} = 7 - 8$ Hz	a,a $\sim$ 8–14 Hz	$^3J_{cis \text{ or } trans} = 4 - 5$ Hz, $n = 5$
$^4J_{meta} = 1 - 3$ Hz	a,e $\sim$ 2–3 Hz	$^3J_{cis \text{ or } trans} = 6 - 10$ Hz, $n = 4$
	e,e $\sim$ 2–3 Hz	$^3J_{cis \text{ or } trans} = 3 - 5$ Hz, $n = 3$

Although, heteronuclear coupling constants can complicate the 1D ^{1}H NMR spectrum, they are not typically observed due to the relatively low natural abundance of ^{13}C (1.1%) and ^{15}N (0.37%). Also, ^{19}F and ^{31}P are not predominant in any given organic compound and do not usually interfere with the interpretation of ^{1}H or ^{13}C NMR spectra.

However, one and multiple bond heteronuclear coupling constants form the basis of heteronuclear two-dimensional (2D) experiments that are extremely useful for structure determination (Keeler, 2005). Specifically, a significant increase in resolution is achieved by dispersing a 1D NMR spectrum into 2D, especially as the complexity of the molecule increases. Secondly, accurately measuring coupling constants can be challenging in complicated 1D NMR spectra that contain overlapping peaks and complex coupling patterns. A typical 2D heteronuclear NMR experiment simply correlates ^{1}H and ^{13}C resonances that are coupled by the observation of a peak that has X,Y coordinates in the 2D spectra equal to the chemical shifts of the coupled resonances in the 1D NMR spectra. For example, a ^{1}H nucleus at 8.31 ppm that is bonded to a ^{13}C nucleus at 132.5 ppm would exhibit a peak in a 2D experiment with X,Y coordinates of 8.31 and 132.5 ppm.

12.4.3 Integration

NMR is a quantitative technique and the integral of each NMR resonance can provide an indication of the number of nuclei associated with each functional group within a compound. The ratios of integrals comparing different signals arising from the same molecule provide an indication of the number of nuclei contributing to each peak. An example of the use of integrals is shown in Fig. 12.5 and some characteristics of integration are summarized in Table 12.3.

If the compound contains impurities or residual solvents, integration of the impurity peak(s) will not yield an integer multiple of the other peaks arising from the major component. This provides a straightforward and easy protocol to identify the peaks associated with the compound of interest and eliminates

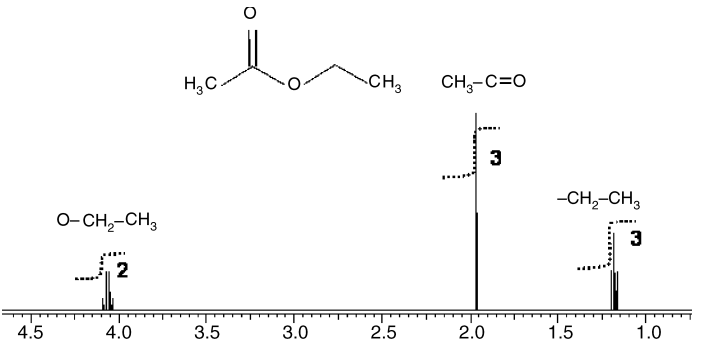

FIGURE 12.5 ^{1}H NMR spectrum with indication of integral for ethyl acetate.

spurious peaks from impurities in the structural analysis. It also provides an approach to quantitate the purity of the compound and the percentage of each impurity present by relative peak integration. A similar approach can be applied to follow dynamic processes, such as the rate of degradation of a compound or chemical exchange between different conformers or isoforms (Sridharan et al., 2005).

12.5 SAMPLE REQUIREMENTS FOR NMR

Traditionally, NMR analysis is performed in high quality NMR tubes using pure compounds and pure deuterated solvents. While this requirement has not changed over the years, the minimum concentration of a compound needed for NMR spectroscopy has been significantly reduced due to the sensitivity enhancements described above. The requirements for metabolite structure determination are the same, but it is often a challenge to obtain sufficient quantities of pure metabolites to conduct traditional NMR measurements. The minimum amount of a metabolite needed for structure determination depends on various factors that include: compound purity, complexity of the structure, the type of biotransformation, 1D versus 2D NMR experiments, and the utility of NMR sample tubes compared to hyphenated NMR approaches such as LC-NMR. With newly emerging cryoprobe technology and probes with lower sample volume (in some cases as low as 30–60 μL), it has become possible to analyze the structure of a metabolite using 1D NMR with a minimum of 500 ng of pure compound. For any detailed follow-up characterization requiring 2D NMR data collection, the amount of pure material needed ranges from 1 μg to several mg, depending on the specifics of the NMR experiments.

In the case of hyphenated NMR methods (Klaus, 2003; Exarchou et al., 2005), compound purification is done online with the structure determination process. This increases throughput and efficiency for analyzing numerous samples prepared in a comparable manner. LC–NMR incorporates a flowprobe that connects the chromatography with the NMR data collection. Simply, as a peak of interest eludes from the HPLC column, the peak continues to travel through additional ''plumbing'' until it is properly positioned in the fixed sample chamber (30–120 μL) in the NMR probe. Generally, the HPLC process is halted (stop-flow) while the NMR data is collected. Alternatively, the NMR data can be collected continuously (on-flow) during the HPLC process, but this is more technically challenging, limits the NMR methodology to quick 1D experiments and requires larger compound concentrations. LC–NMR requires an HPLC method that can separate the compound of interest in high enough concentration, where the solvent system also needs to be compatible with NMR data collection and analysis. In addition to good separation, the quality of deuterated or protonated solvents used for HPLC, the stability of HPLC columns and prior knowledge of retention time and the molecular weight are all crucial for metabolite identification using LC–NMR.

12.6 MOST COMMONLY USED NMR EXPERIMENTS AND TECHNIQUES

Four general classes of NMR experiments are routinely used to analyze metabolites: (1) 1D NMR experiments; (2) 2D NMR experiments; (3) Solvent suppression methods; and (4) Hyphenated NMR experiments. The 1D and 2D NMR experiments are commonly used for metabolite structure determination. The various solvent suppression techniques (Gaggelli and Valensin, 1993; Hwang and Shaka, 1995; Smallcombe and Patt, 1995) are crucial for dilute metabolite samples where the solvent peak is the most intense peak in the NMR spectrum. These solvent suppression techniques can be incorporated as needed in both 1D and 2D NMR experiments. Since their introduction in the 1990s, hyphenated NMR methods have become common tools in the identification of metabolites. These methods include LC–NMR (Albert, 1995; Spraul et al., 1993, 1994), LC–NMR–MS (Mass Spectrometry) (Shockcor et al., 1996) and LC/SPE (solid phase extraction)/NMR (Alexander et al., 2006; Bieri et al., 2006; Xu et al., 2005; Wilson et al., 2006).

12.6.1 1D NMR Experiments

A simple 1D NMR spectrum can offer rich structural information for metabolites. For example, a ^{1}H NMR spectrum identifies the functional groups present in the metabolite structure from ^{1}H chemical shifts, determines the structural connectivity of these functional groups from coupling patterns and coupling constants, provides a relative atom count from peak integrals, and suggests the number and type of exchangeable hydrogens from broadened peak widths. The main disadvantage of 1D ^{1}H NMR spectroscopy is signal overlap due to the narrow dispersion of ^{1}H chemical shifts.

Correspondingly, a 1D ^{13}C NMR spectrum overcomes the ^{1}H NMR resolution problem and is complimentary to ^{1}H NMR. The typical chemical shift range of a ^{13}C NMR spectrum is $\sim$220 ppm compared to 15 ppm for ^{1}H NMR spectrum. Also, a number of carbon types (carbonyl, carboxylic acid, aromatic, etc.) are not observable in a ^{1}H NMR spectrum because of the lack of attached hydrogen(s). The major disadvantage of ^{13}C NMR spectroscopy is its extremely low sensitivity compared to ^{1}H NMR experiments. This occurs because of the low natural abundance of ^{13}C nuclei (1.1%) and the low magnetogyric ratio ($\gamma^{1}H/\gamma^{13}C$). As a result, a ^{1}H NMR spectrum is $\sim$64,000 times more sensitive than a ^{13}C NMR spectrum. Also, because of the low ^{13}C abundance, ^{13}C NMR spectra are generally collected in a "decoupled" mode, which removes the strong (and generally uniform) one bond $^{1}H-^{13}C$ coupling. This increases the sensitivity of a ^{13}C NMR spectrum and reduces its complexity removing peak splitting, but it also eliminates the important bond connectivity information that is valuable for metabolite structure determinations.

In general, both 1D ^{1}H and ^{13}C NMR spectra are collected to resolve a metabolites structure. 1D NMR spectra of other heteronuclei (^{15}N, ^{19}F, ^{31}P)

are only collected to verify their presence in the metabolite or to greatly simplify the interpretation of the NMR spectra since these 1D heteronuclear NMR spectra typically only contain a few peaks.

A 1D nuclear overhauser experiment (NOE) (Gaggelli and Valensin, 1993) is an important and valuable variation on the simple 1D NMR experiment that provides spatial relationship between each nucleus in the structure. Coupling constants observed in a 1D ^{1}H NMR spectra provide connectivity for directly bonded nuclei; whereas, a 1D NOE experiment identifies nuclei that are close in space (≤ 6 Å). Briefly, a 1D NOE experiment requires the addition of a second lowpowered rf pulse that selectively "saturates" a specific peak in the NMR spectrum. The saturated peak becomes a null in the spectrum and any other nuclei that are coupled through space via a dipole–dipole interaction to the saturated peak will experience a change in peak intensity. A 1D NOE experiment requires collecting two NMR spectra, with and without saturation, to monitor changes in peak intensity. A summary of common 1D NMR experiments and their applications are listed in Table 12.6.

12.6.2 2D NMR Experiments

A fundamental component of the interpretation of NMR data is deciphering the NMR assignments, which correlates an observable NMR resonance with a specific atom in the molecular structure of the metabolite. This process is illustrated using the structure and ^{1}H NMR spectrum of 1,3-dimethylnaphthalene as an example (Fig. 12.6). The two methyl groups have distinct ^{1}H NMR chemical shifts because of their unique local environments. The NMR assignment process results in attributing the NMR peak at 2.57 ppm to methyl (a) and NMR peak 2.39 ppm to methyl (b).

The 1D NMR experiment provides the basic information, chemical shifts, coupling constants, and peak integration required for assigning NMR spectra, 2D experiments have become common for complete structure determination of organic compounds, natural products, and metabolites. 2D NMR experiments are generally used to confirm assignments derived from 1D NMR experiments, to resolve spectral ambiguities and provide new assignments that were not apparent in the 1D NMR experiments because of peak overlap or complex coupling patterns, and to provide $^{1}H-^{1}H$ and $^{1}H-^{13}C$ correlations that help confirm the structure of a compound.

2D NMR experiments have two important advantages over 1D NMR experiments. First, 2D NMR experiments provide a significant increase in resolution from the added dimensionality, which helps in resolving overlapped resonances in 1D NMR spectra. Second, 2D NMR experiments contain additional information that directly correlates NMR resonances that are coupled either through bonds or through space. Generally, a 2D NMR experiment contains a diagonal that corresponds to the standard 1D NMR spectrum. Diagonal peaks are correlated by off-diagonal "crosspeaks" that arise from a coupling constant or an NOE. A major disadvantage of 2D NMR

TABLE 12.6 Common 1D NMR experiments and their characteristics.

1D NMR experiment	Application	Advantages	Limitations	Comments
1D ^{1}H	Verify or eliminate proposed structures by comparing the changes in chemical shifts, coupling constants, and integrations with that of the parent molecule.	Simple, fast, and highly sensitive. It can be observed on a sample as little as 0.5 μg.	Signal overlaps cannot be resolved. Can not differentiate HC−O from HC−N or HC−O from CH=CR	Should be used as the first experiment for any meta bolite ID work when compared to its parent molecule
1D ^{1}H with solvent suppression	Same as above.	Improve the sensitivity of the proton spectrum for which the solvent signals is extremely strong	In addition to the above some resonances may not be observed due to overlap with solvent resonances	Should be used when the solvent signal is strong and when the sample concentration is very low
1D NOE	It provides stereochemistry information Some times, it is used to verify connectivity of the molecule.	Extremely powerful for stereochemistry determination and connectivity verification	Low sensitivity, stable spectrometer required for long data collection, >20 μg of compound required	Use only where required or appropriate

(*continued*)

TABLE 12.6 (*Continued*)

1D NMR experiment	Application	Advantages	Limitations	Comments
1D ^{19}F	Verify the modification site is near or at the fluorine atom. Verify the relative ratio of total metabolites.	High sensitivity. It could provide additional structure information when the sample amount is limited for other NMR experiment. Can be used for mass balance issues	Limited applications	Use for compounds containing ^{19}F.
1D ^{13}C	Verify carbon skeleton and functional group modifications in the molecule.	Chemical shifts provide characteristic range for different functional groups. It is a powerful tool to distinguish C−N versus C−O and C−O versus C=C	Insensitive, >100 μg sample required for reasonable spectra	Rarely performed on isolated metabolites due to sample limitations

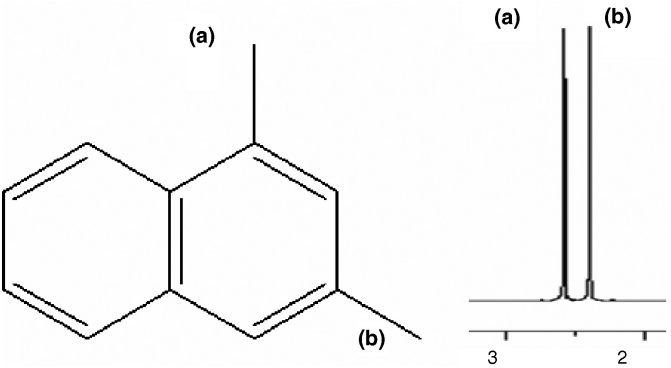

FIGURE 12.6 1,3-Dimethylnaphthalene structure with NMR assignments of methyl resonances.

experiments is the increase in experimental time (hours–days) compared to minutes for a typical 1D NMR spectrum. Also, 2D NMR experiments have a higher sample requirement ($\geq$1 μg) because of the inherently lower sensitivity. Some common 2D NMR experiments that are routinely used for structure characterization of metabolites are described in Table 12.7.

12.6.3 Solvent Suppression Techniques

A significant concentration difference between the compound and the solvent (deuterated and protonated) may create a large dynamic range problem for an NMR experiment since the NMR signal intensity is proportional to concentration. Thus, dilute metabolite samples require NMR experiments that can suppress the relatively intense solvent peaks. This issue is further aggravated in cases of metabolite structure determination due to challenges in isolating critical metabolites from biological systems in sufficient quantities and purity for NMR analysis. In some cases, the dynamic range difference between the solvent and the metabolite is close to 1000 : 1 ratio. This large difference in signal intensity results in the saturation of the receiver, where only the solvent signal is observed. The signals from the metabolite are lost in the baseline because of the digital limitations of the receiver (Fig. 12.7).

To address the solvent dynamic range problem, one or multiple signals from the solvent are *selectively* suppressed in the NMR spectrum. Solvent suppression is not a perfect solution. Compound peaks that are proximal to the solvent are also completely or partially suppressed. Similarly, hydrogens that readily exchange with water are also equally suppressed with the water solvent peak. Additionally, solvent suppression causes artifacts and streaking in 2D NMR spectra. This streaking may obscure cross peaks that fall near the solvent chemical shift in either spectral dimension. The commonly used solvent suppression NMR techniques, such as, PRESAT, WET (Smallcombe and Patt,

TABLE 12.7 Common 2D NMR experiments and their applications.

2D NMR experiment	Application	Advantages	Limitations	Comments
COSY (correlated spectroscopy)	Provides 2 and 3 bond $^{1}H-^{1}H$ connectivity	Simple to run, resolves overlapped proton resonances. Minimum amount required 1–2 μg	Greater than three bond correlations cannot be observed	Any ambiguity in the 1D ^{1}H assignment should be followed by a COSY
TOCSY (total correlated spectroscopy)	Provides 2, 3, 4 and 5 bond $^{1}H-^{1}H$ correlations	Simple to run, provides long through-bond connectivites. Minimum amount required 2–5 μg	Sometimes, some long bond correlation may not be observed. High power may be required for the spin lock pulse	Confirms the COSY as signments or can be performed instead of a COSY. Used for identifying contiguous proton spin systems
NOESY (NOE spectroscopy)	Reveals through space interactions	Stereochemical questions can be answered for appropriate molecules	Not a simple experiment to perform. Data can be complicated due to exchange peaks Insensitive	Only used where appropriate
ROESY (rotating frame noe spectroscopy)	Same as NOESY, through-space interactions	Same as NOESY plus can distinguish between exchange and ROE peaks	Same as NOESY and also insensitive	Same as NOESY
HMQC (heteronuclear multiple quantum correlation) or HSQC (heternuclear single quantum correlation)	Provides 1 bond $^{1}H-^{13}C$ or $^{1}H-^{15}N$ correlation	Can identify all the protonated carbons and nitrogens in a molecule	Less sensitive experiment due to low sensitivity of ^{13}C and ^{15}N Compound requirement is high Minimum 20 μg or more	Can assist in identifying complete unknowns, unexpected products or metabolites
HMBC (heteronuclear multiple bond correlation)	Provides 2 to 3 bonds $^{1}H-^{13}C$ and $^{1}H-^{15}N$ correlation.	Crucial for identifying nonprotonated carbons and nitrogens	Most insensitive experiment. 100 μg and higher amount of material required	Useful for complete unknowns, unexpected products and metabolites

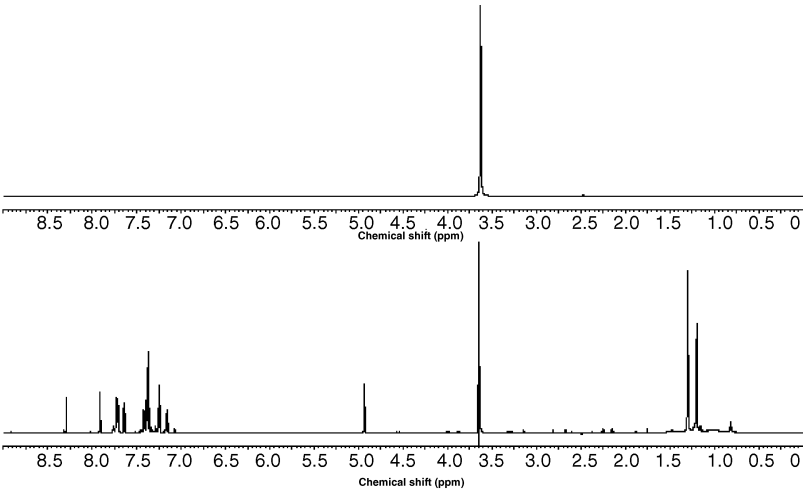

FIGURE 12.7 1D ^{1}H spectrum of a metabolite sample in DMSO-d_6, with and without solvent suppression. Regular single pulse sequence (top). WET sequence used to suppress residual H_2O and DMSO signals (bottom). The NMR spectra are plotted on the same scale.

1995) and excitation sculpting (Hwang, 1995) and their advantages and disadvantages are listed in Table 12.8.

12.6.4 Hyphenated NMR Methods

High performance liquid chromatography has played a major role in the separation and purification of compounds, especially in the pharmaceutical industry. With the introduction of NMR flowprobes in late 1990s (Albert, 1995), it became possible to link HPLC directly to a NMR flowprobe and introduce HPLC separated fractions directly into an NMR spectrometer for analysis. The LC–NMR combination provides a unique advantage for unstable metabolites by permitting real time monitoring of the purification and structure analysis process. Since the introduction of LC–NMR (Lindon et al., 1996), several additional hyphenated techniques LC–MS–NMR (Shockcor et al., 1996; Yang, 2006), and LC–MS–SPE–NMR (Alexander et al., 2006; Bieri et al., 2006; Xu and Alexander, 2005; Seger et al., 2006; Wilson et al., 2006), have been introduced that are now routinely used in the pharmaceutical industry to support the characterization of metabolites and impurities.

MS provides the added capability of identifying a molecularweight to an unknown metabolite chromatographic peak, which significantly simplifies the NMR structural analysis. Similarly, solid-phase extraction addresses a common limitation of hyphenated techniques. NMR is an inherently insensitive technique requiring a large sample size ($\geq$500 ng) to observe a simple 1D NMR spectrum, which may not be achieved for biological

TABLE 12.8 Common solvent suppression methods.

Suppression sequence	Setup	Advantages	Limitations
Presaturation	Traditionally, the solvent signal is irradiated for a period of time with a continuous wave rf field	Can be easily set up Useful for eliminating single solvent signal.	Extremely sensitive to spectrometer stability and shimming. Not easy to suppress multiple solvent peaks simultaneously. Also, suppresses exchange peaks Suppresses NMR signals from the compound that overlaps with the solvent.
Excitation sculpting	The solvent resonances are extracted from the spectra with selective pulses	Involved setup, could be automated, exchange resonances are not suppressed, multiple solvent peaks can be suppressed. Extremely flat baselines.	Setup is involved. Several elements in the pulse sequence need to be optimized Suppresses NMR signals from the compound that overlap with the solvent
Watergate exitation technique (WET)	The solvent resonances are selectively suppressed at the beginning of the NMR experiment. This pulse sequence is the most widely used solvent suppression technique for LC–NMR experiments	Involved setup, could be automated, exchange resonances are not suppressed, multiple solvent peaks can be suppressed. ^{13}C decoupling	Suppresses NMR signals from the compound that overlaps with the solvent Baseline distortions

metabolites in the LC–NMR mode. SPE provides a simple approach to collect and concentrate individual HPLC peaks prior to NMR analysis. The purified compound is extracted from an SPE column in a small volume (~30 μL) and can be further concentrated by collecting peaks from multiple HPLC injections. This also reduces the amount of deuterated solvents used, since only a small volume (~300 μL) of solvent is required to elude the compound from the SPE column.

The most common HPLC solvents used for LC–NMR are acetonitrile and water. Both protonated and deuterated acetonitrile and water are commercially available and routinely used, where cost is a major consideration in minimizing the utility of deuterated solvents in HPLC experiments. Commonly, a low percentage of trifloroacetic acid (TFA) is also added to the HPLC solvent system to improve the LC peak lineshape. In some cases, a methanol–water solvent mixture replaces the water–acetonitrile system if the compound of interest does not behave well (low solubility, aggregation, broad peak shape). If an MS system is attached to the LC–NMR to monitor the molecular weight than formic acid is preferred as a modifier. Table 12.9 provides a list of commonly used hyphenated techniques and their advantages and disadvantages.

The LC–NMR component of hyphenated systems can be performed in three different modes; on-flow, stop-flow and loop storage/transfer. In the on-flow mode, the NMR spectra are collected continuously at predefined intervals during the chromatographic run. The NMR experiments are typically limited to simple 1D ^{1}H NMR experiments that can be rapidly collected during the limited time. Also, NMR spectra may contain multiple compounds since there is no correlation between peak elution and NMR data collection. An NMR spectrum could be collected during the time period when one peak is finishing eluting from the column and a second peak has started eluting from the column. So, both compounds are present during some fraction of the NMR data collection time.

Conversely, stop-flow stops the chromatography after a specific peak has eluded and the compound has been transferred to the NMR flowprobe. This enables longer, more complicated NMR experiments to be collected on a pure metabolite. The major disadvantage of this mode occurs if multiple metabolites are analyzed. The compounds and the chromatographic peaks still remaining on the HPLC column may deteriorate during the NMR data collection time. The loop storage/transfer mode is similar to stop-flow except for the inclusion of a SPE column to concentrate the sample prior to NMR analysis. The loop storage/transfer mode has similar issues regarding compound stability. The three modes and their advantages and limitations are highlighted in the Table 12.10.

12.7 GENERAL PROTOCOL FOR NMR ANALYSIS OF UNKNOWN COMPOUNDS OR METABOLITES

The application of NMR for the analysis of metabolite structures is a multi-step process that is fundamentally based on spectral comparisons. The first step

TABLE 12.9 Advantages and limitations of the most common hyphenated NMR methods.

Technique	Setup	Advantages	Limitations
LC–NMR	HPLC system connected to the NMR flow probe (30–120 μl) via a UV detector. Experiments can be performed in on-flow, stop-flow, and loop collection modes DAD UV detector used for peak detectionRegular reversed-phase C18 (4.6 × 150 mm) columns CH_3CN or CH_3OH:H_2O with trifloroacetic acid or formic acid as a modifier. At least one of the solvents is deuterated.	Eliminates the need for sample isolation and purification associated with regular tube NMR Useful for analysing compounds that may degrade during isolation Isocratic and gradient HPLC methods can be used	Use of deuterated solvents for LCSample limited to column size, NMR flow cell and chromatographic resolution Solvent suppression techniques are necessary even when both solvents are deuterated Need for NMR friendly solvent modifiers Disconnect between UV and MS retention time due to the use of two separate instruments
LC–NMR–MS	20 : 1 flow splitter added after the LC column resulting in 5% of the flow going into the MS source and 95% going into the NMR flow cell All three modes can be performed	Disconnect between the UV and MS retention times are addressed MS and MS/MS data can be collected during analysis Can be used to determine number of exchangeable protons in the metabolite	Need for MS friendly solvent modifier (i.e., formic acid) Complex setup. Maintenance of the hardware is time consuming

LC-SPE-MS-NMR	HPLC system connected to a solid phase extraction (SPE) system Compound of interest is ''trapped'' in a SPE cartridge and later transferred into the NMR flow probe for analysis MS can be used during the LC analysis and during the analysis of the cartridge	Fraction of interest is concentrated in the cartridge prior to the NMR analysis Chromatography can be performed using protonated solvents with any modifier Sample is loaded into the NMR flow cell using deuterated solvents minimizing the need for solvent suppression Various solid phase options available in SPE cartridge to optimize for different compounds	Not all compounds can be trapped into the SPE cartridge, limiting its use with certain type of compounds Complex setup. Maintenance of the hardware is time consuming

TABLE 12.10 Advantages and limitations of the common LC–NMR–MS methods.

Mode	Setup	Advantages	Limitations
On-flow	In this mode the HPLC column is connected directly to the NMR probe via a DAD detector A series of 1D spectra are collected with a predefined number of scans without stopping the chromatographic experiment	Provides a metabolite profile of the sample Can be used with ^{1}H and ^{19}F to monitor metabolite degradationWith ^{19}F monitoring, as most of the peaks observed are from the compound solvent suppression is not needed	Limited to compounds with on column loadings $>10\ \mu g$ Limited to 1D NMR experiments.Broadening of the NMR signal due to on-flow conditions Solvent suppression is a challenge due to solvent gradients used for LC
Stop-flow	In this mode the LC chromatography is temporarily stopped at the peak of interest using the UV or MS (LC–NMR–MS) signal	Detailed structure determination can be performed on the peak of interest by performing 1D and 2D NMR	The LC peak shapes deteriorate for the latter peaks of interest
	The timing between the UV or MS detector and the NMR flow cell is critical. Either the UV or the MS signal can be used to pause the LC run.	>100 ng for ^{1}H experiments and $>1\ \mu g$ for 2D $^{1}H-^{1}H$ experiments is required.	LC peaks of interest must be well resolved. >2 min retention time differenceCross contamination from various LC fractions

TABLE 12.10 (*Continued*)

Mode	Setup	Advantages	Limitations
Loop-storage or SPE/transfer	LC chromatography is performed first with collection of peaks in a loop cassette or SPE cartridge using the UV or MS signals The stored fractions in the loops or SPE are then transferred into the NMR flow probe for analysis Computer control of the instrument is essential in this mode of operation	LC chromatography could be performed independently from the NMR experiments Since the chromatography is not stopped, issues with peak broadening in the stop-flow mode are eliminated. Eliminates cross contamination problems Multiple experiments on each sample are possible including Heteronuclear experiments such as $^{1}H-^{15}N$	Sample could decompose during the storage period Requires the use of special equipment to direct the flow through different pathways

of metabolite structure identification is to assign all the ^{1}H and ^{13}C NMR resonances of the *parent compound* to the corresponding atoms in the molecular structure. This is accomplished using the complete repertoire of 1D- and 2D-NMR experiments discussed in detail in Sections 12.6.1 and 12.6.2. The next step of the process is to compare the ^{1}H NMR spectrum of the metabolite to the corresponding NMR spectrum for the parent compound.

From this spectral comparison, it is relatively straightforward to identify key changes in chemical shift (e.g., upfield versus downfield), coupling patterns (e.g., doublet versus triplet), coupling constants (e.g., 2 Hz versus 8 Hz), peak integration (e.g., 1 H versus 2 H) and the disappearance or appearance of peaks in the metabolite NMR spectrum. The third step is to link these NMR spectral changes to specific site(s) on the parent molecule's structure. (Are these changes on an aromatic ring or near an alkene double bond?) In most cases, the comparison of 1D spectrum, combined with MS spectral analysis, provides preliminary answers or inferences to the location and type of modifications that occur between metabolites and the parent compound. These preliminary results can be confirmed by performing 2D NMR experiments that specifically address issues identified from the 1D NMR analyses.

The application of NMR to analyze metabolite structures is illustrated using a 6-hydroxy buspirone as an example. Figure 12.8 shows the ^{1}H spectrum of 6-hydroxy buspirone. It is clear from the complexity of the 1D ^{1}H NMR spectrum, that the primary structure of 6-hydroxy buspirone could not be easily determined by only using 1D NMR data. The 2D homonuclear experiments, TOCSY (Figs. 12.9 and 12.10) and DQF–COSY (Fig. 12.11), were collected on 6-hydroxy buspirone to identify ^{1}H NMR resonances that are coupled and correspondingly chemically bonded. The spin systems for protons 7–10 were identified by the combination of coupling patterns observed in both the TOCSY and DQF–COSY spectra. The spin system and coupling pattern are highlighted in both NMR spectra. The ^{13}C chemical shifts were determined from 2D heteronuclear data, HSQC and HMBC, as shown in Figs. 12.11 and 12.12, respectively. The 2D $^{1}H-^{13}C$ HSQC spectrum shows cross peaks for all one bonded $^{1}H-^{13}C$ pairs. The ^{13}C NMR assignments for all protonated carbons are obtained by simply correlating the assigned ^{1}H NMR resonances with a corresponding ^{13}C NMR resonance by the cross peaks observed in the 2D $^{1}H-^{13}C$ HSQC spectrum (Fig. 12.10).

The HMBC experiment correlates long-range (two to three bond) $^{1}H-^{13}C$ pairs (Fig. 12.11) three is used to determine the ^{13}C chemical shifts and structural connectivity of quaternary and carbonyl carbons. Quaternary and carbonyl carbons do not have directly bonded hydrogens and as a result do not have a cross peak in the 2D $^{1}H-^{13}C$ HSQC spectrum. Fig. 12.11 shows cross peaks for the correlation between hydrogens 10 and 13 with carbonyl carbon 12, and hydrogen 20 with carbonyl carbon 19. Also shown in the HMBC spectrum is the correlation between hydrogens 23 and 25 with quaternary carbon 21. Despite a lack of correlations to spiro-carbon 14, the overwhelming body of evidence from interpretations of multiple NMR

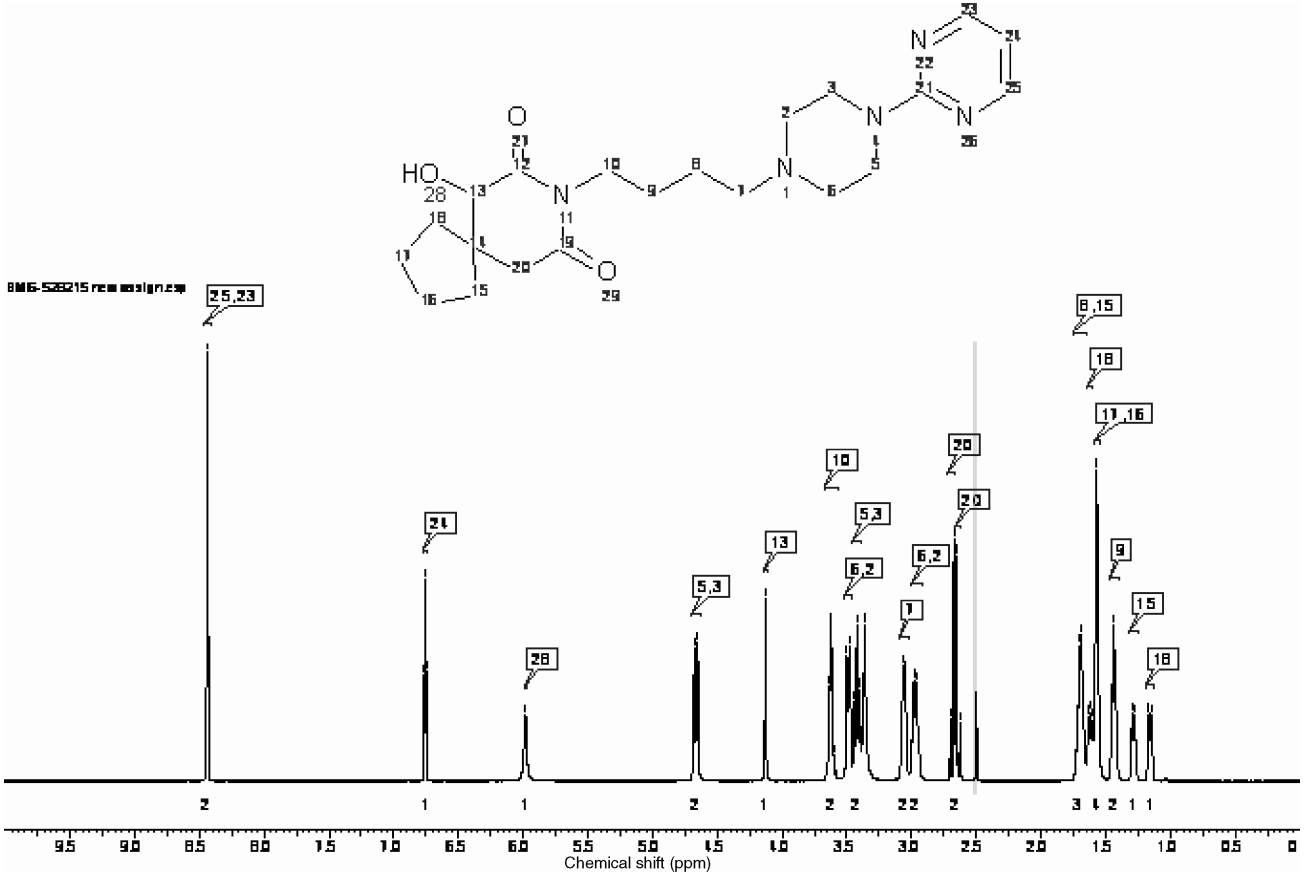

FIGURE 12.8 ^{1}H spectrum and its assignment of 6-hydroxy Buspirone in DMSO.

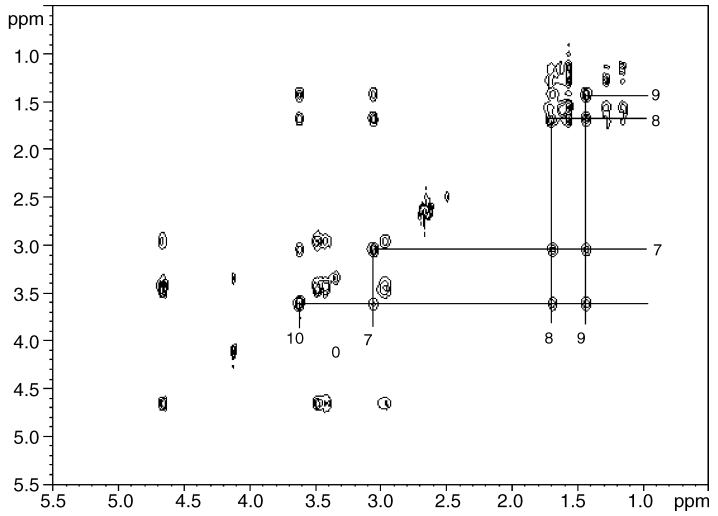

FIGURE 12.9 2D $^{1}H-^{1}H$ TOCSY spectrum of 6-hydroxy buspirone.

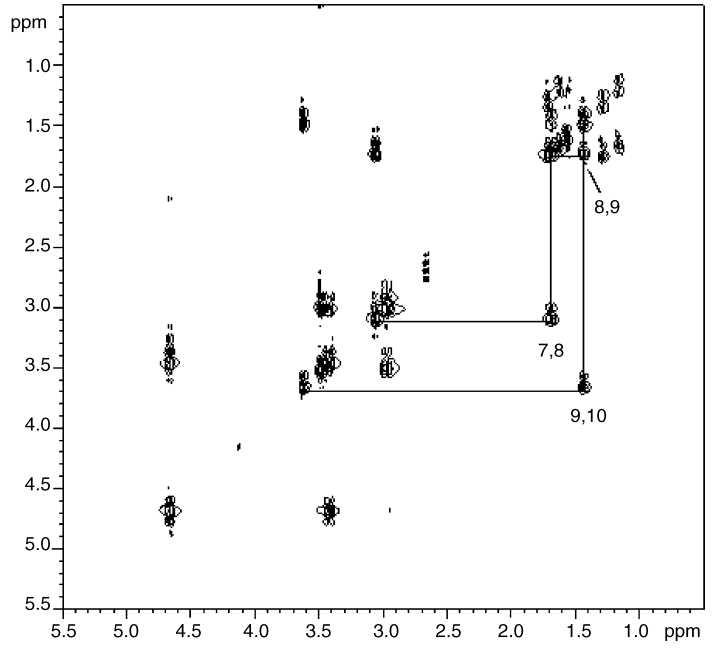

FIGURE 12.10 2D $^{1}H-^{1}H$ DQF–COSY spectrum of 6-hydroxy buspirone.

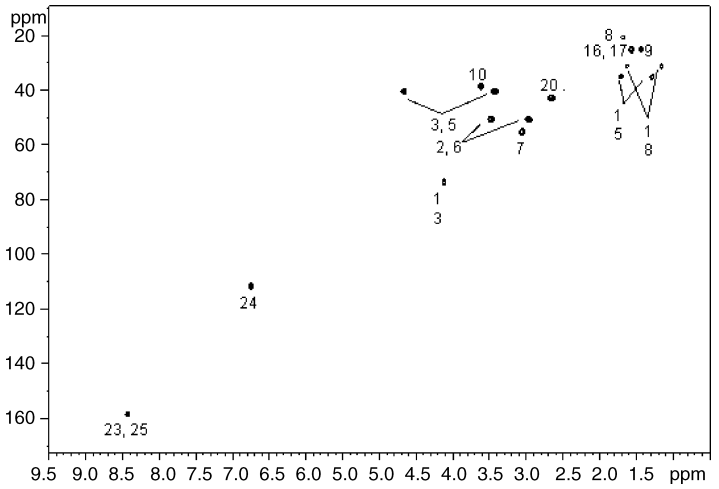

FIGURE 12.11 2D $^{1}H-^{13}C$ HSQC spectrum of 6-hydroxy buspirone.

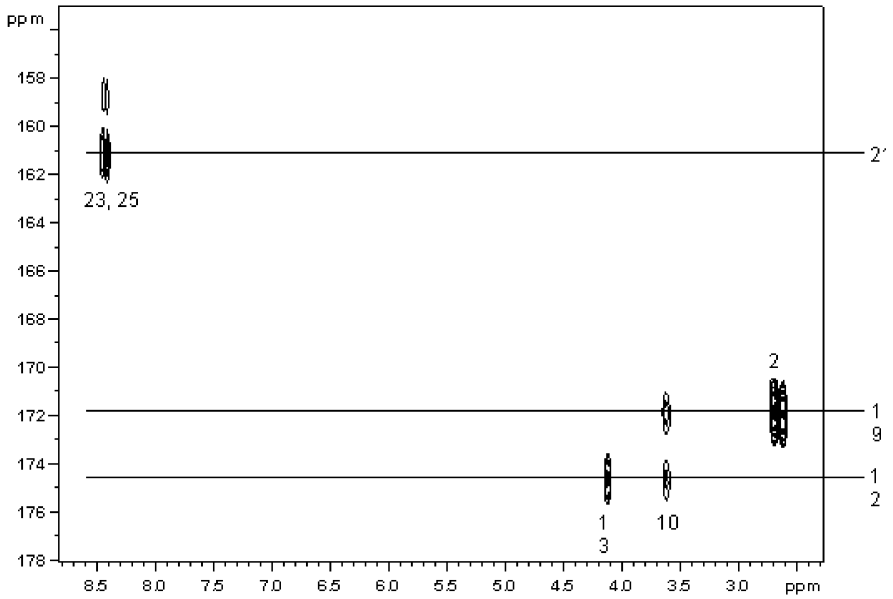

FIGURE 12.12 2D $^{1}H-^{13}C$ HMBC spectrum of 6-hydroxy buspirone (carbonyl region).

TABLE 12.11 Metabolite identification by using NMR spectroscopy.

Metabolic reaction	Metabolite identification examples	NMR indications	Confirmation method and comments
1. Dealkylation	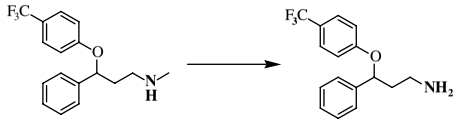 Fluoxetine Nor fluxetine	The methyl group at δ2.98 (s, 3H) disappeared The α-CH_2 group shifted from δ2.82 to δ2.98 ppm	There is no need for further confirmation
2. Aliphatic hydroxylation (Gerhard et al., 2003)	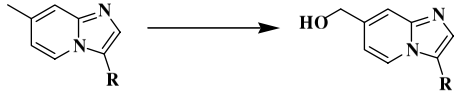	The methyl group at δ2.45(s, 3H) disappeared A new peak appeared at δ4.71 ppm (s, 2H), which is characteristic for a methylene alcohol	There is no need for further confirmation
(Chando et al., 1998)	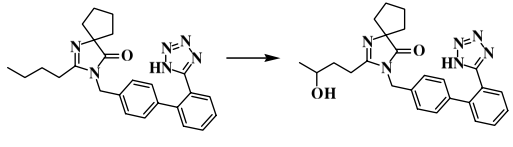 Irbesartan hydroxyl-irbesartan	The methyl proton shifted from δ0.80 to δ1.00 ppm and its coupling pattern changed from a triplet to a doublet The α-CH group shifted from δ1.23 (m, 2H) to δ3.58 (m, 1H), which is consistent with a secondary alcohol	The methyl and methine groups indeed belonged to the same spin system could be confirmed by the 2D COSY experiment

3. Aromatic hydroxylation (Gerhard et al., 2003)	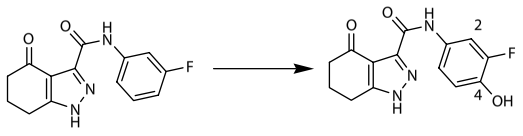	The hydroxylation position at C2 or at C4 was not obvious from the 1D proton spectrum due to the presence of the F−H couplings 2D COSY spectrum indicated the larger doublet at δ7.25 (8.1 Hz) was due to vicinal coupling of F−H while the smaller coupling (2.3 Hz) was the result of H2−H6 meta coupling Based on the coupling constant, the hydroxylation occurred at the C4 position	No further experiment is needed to confirm the regiochemistry
4. Epoxidation (Garcia et al., 2004)	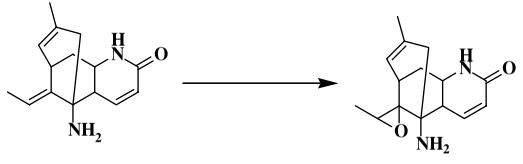 Huperzine A 13,14-Epoxy Huperzine A	The olefinic protons shifted from δ6.12 to δ2.79 ppm. This observation is characteristic for epoxide in which the proton normally appears at δ2.2–2.9 ppm	The formation of epoxide can be confirmed by determining the shifts of C13 and C14 carbons involved in epoxide formation either by performing $^{1}H-^{13}C$ HMQC or direct ^{13}C 1D experiments. Both carbons should shift from ~130 to ~50 ppm.

(*continued*)

TABLE 12.11 (*Continued*)

Metabolic reaction	Metabolite identification examples	NMR indications	Confirmation method and comments
5. *N*-oxidation (Jairaj et al., 2002)	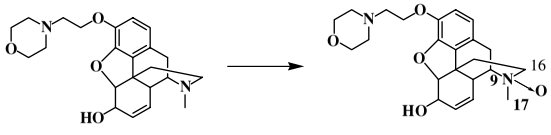 Pholcodine → Pholcodine-N-Oxide	The large downfield carbon ($\Delta\delta > 12$ ppm) and proton ($\Delta\delta > 0.6$ ppm) shifts for C16, C17, and C9 were indicative of N–oxide formation at the *N*15 nitrogen (chemical shifts changes are listed in the Table 12.12)	The N-oxidation position could be confirmed by ^{15}N HMBC experiment. The downfield 10–30 ppm nitrogen shift is indicative of the *N*-oxide. However, this experiment requires >100 μg of sample
6. *S*-Oxidation and *S*-reduction	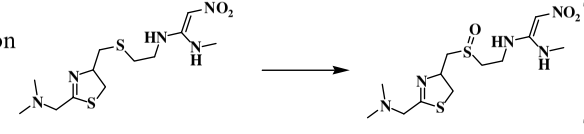 Nizatidine → Nizatidin Sulfoxide	The methylene carbons that connected to the sulfur group shifted from ~35 to ~52 ppm The α-methylene protons shifted from ~2.3 to ~3.0 ppm	There is no direct NMR method to confirm the existence of the sulfoxide group as sulfur is not an NMR active nucleus
7. Alkene reduction	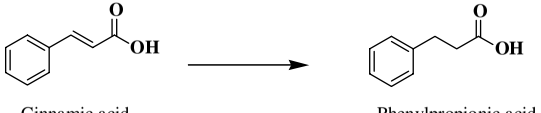 Cinnamic acid → Phenylpropionic acid	The olefinic protons shifted from 6.36 and 7.73 to 2.59 and 2.89 ppm, respectively The coupling pattern changed from large doublet (14.8 Hz) to the smaller multiplets The integration of the corresponded signals increased from one proton to two protons	The alkene reduction can be further confirmed by observing the changes in the carbon shifts from 110–140 ppm to about 30 ppm by performing an $^{1}H-^{13}C$ HMQC experiment

8. Glutathione conjugation (Dagnino-Subiabre et al., 2000)	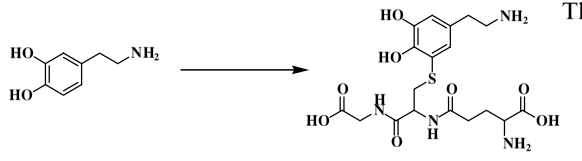	The C-5 aromatic proton was missing and the coupling pattern of the remaining two aromatic protons changed to a 1.8 Hz doublet The β-methylene of the cysteine shifted from 2.87 to 3.10 ppm	The position of the GSH attachment could be confirmed by an NOE experiment. NOE may be observed between the β-methylene of the cysteine and the aromatic C4 proton. The $H1-C13$ HMBC experiment may also help. This experiment requires require >100 ug of the metabolite
9. Methylation (Basker et al., 1990)	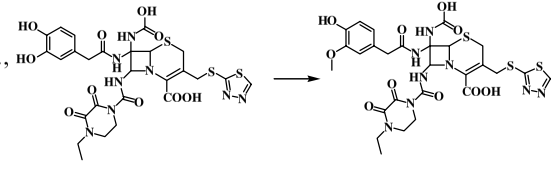 Analog of Catecholic Cephalosporin	A new sharp methoxyl signal at δ3.86 (s, 3H) ppm was observed	The structure was confirmed by HMBC and NOE experiments
10. Sulfation (Daykin et al., 2005)	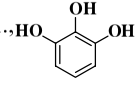 Pyrogallol 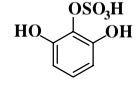 dihydroxyphenyl-2-O-sulfate	All three aromatic protons shifted slightly downfield. H4 and H6 protons shifted by 0.10 ppm and the H5 shifted by 0.21 ppm The aromatic protons of the metabolite showed two groups of signals as did the parent compound, which is consistent with the symmetrical metabo lite formed by sulfation at the C2 hydroxyl	No further experiments can be performed due to lack of NMR active nuclei in the $-SO_3H$ group.

(*continued*)

TABLE 12.11 (*Continued*)

Metabolic reaction	Metabolite identification examples	NMR indications	Confirmation method and comments
11. Hydrolysis	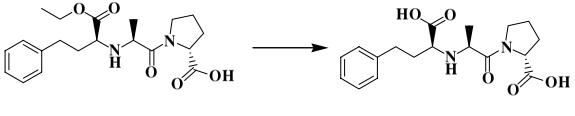 Enalapril Enalaprilate	The ethylene protons (δ4.5, q, 2H; δ1.2, t, 3H) disappeared from the proton spectrum of the Enalaprilate and the rest of the protons and the spin system were intact	There is no need for confirmation
12.Glucuronide conjugation (Froehlich et al., 2005)	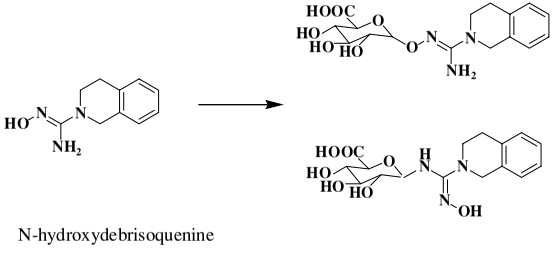 N-hydroxydebrisoquenine	The O versus N-glucuronidation was not determined from the proton spectrum as the anomeric protons for both of the regio isomers were in the 4.5–6 ppm range.	However, measurement of anomeric carbon chemical shifts provided the answer due to significant chemical shift differences between the O-glucoronide (100–110 ppm) and the N-glucoronide (80–90 ppm).
(Zhang et al., 2004)	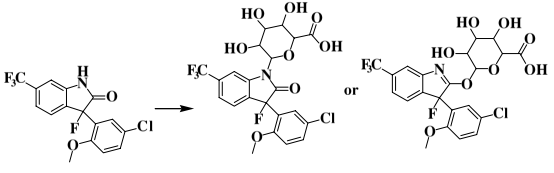 BMS-204352 Confirmed	The carbon chemical shift (δ82.9 ppm) for the anomeric carbon C1′ was indicated from the HMQC experiment, which is consistent with the N-conjugation	The N-glucuronide structure was confirmed by the HMBC experiment. Observation of the long range H–C correlation from the anomeric proton to the indolinone carbonyl supported the *N*-glucuronide conjugation

13.Amino acid conjugation	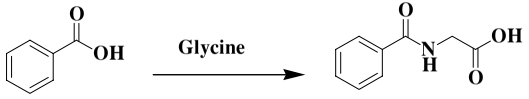 Benzoic Acid Hippuric Acid	The proton signal for the methylene proton was at δ4.3 ppm, compared with the same proton for glycine at δ3.8 ppm The amide proton (δ9.4, t, 1H) was also observed All the aromatic protons were present Integration of all the peaks was consistent	No further experiments are needed

spectral data sets led to the establishment of the metabolite structure as 6-hydroxy buspirone.

12.8 EXAMPLES OF METABOLITE STRUCTURE DETERMINATION FROM KNOWN BIOTRANSFORMATIONS

The availability of the chemical structure and NMR assignment s for the parent compound, as illustrated in Section 12.7 for Buspirone, significantly simplifies the identification of related metabolites. A significant amount of information has already been accumulated and presented in the literature that describes numerous metabolic reactions associated with a variety of metabolic pathways. Examples of the most common metabolic reactions are tabulated in Table 12.11. These metabolic reactions identify a range of possible chemical modifications that may be applied to the parent compound and generate a variety of related metabolites.

The metabolites that are generated from the parent compound can be viewed as simply incurring an addition and/or subtraction of functional groups while maintaining most of the intact parent structure. Similarly, the addition and/or subtraction of functional groups will result in corresponding changes in the NMR spectra, while the majority of the NMR spectrum is unperturbed relative to the parent compound. Again, the comparison of the NMR spectra between the parent compound and the metabolite will easily highlight these structural changes while confirming the parts of the structure that are unaffected. Representative NMR methods to determine the structure of metabolites resulting from various metabolic reactions have been described in the literature and are also listed in Table 12.11.

Occasionally, xenobiotics undergo metabolic activation to produce reactive intermediates, where these intermediates rearrange to form an unpredictable metabolite. For example, the metabolic activation of DPC 963 in rat formed a highly reactive oxirene intermediate (Chen et al., 2002). This intermediate rapidly rearranged to form an unstable cyclobutenyl ketone through possible intermediates a or b (Fig. 12.13). This reactive intermediate was prone to nucleophilic attack and in this case reacted with glutathione via a 1,4 Michael addition that resulted in two isomeric GSH adducts M3 and M4. The ^{1}H NMR spectrum provided evidence in support of the M3 and M4 structures. First, both the aromatic hydrogens were still present in the metabolite. Second, the

TABLE 12.12 Proton and carbon chemical shifts of pholcodine and its *N*-oxide metabolite.

Protons	Parent	*N*-oxide	$\Delta\delta$	Carbons	Parent	*N*-oxide	$\Delta\delta$
δH-16	2.35, t 2.72 dt	3.25, t, 3.38, dt	0.66–0.90	δC-16	47.5	60.4	12.9
δH-17	2.58 s	3.44, s	0.86	δC-17	43.2	58.5	15.3
δH-9	3.31, dd	3.92, dd	0.61	δC-9	60.2	75.9	15.7

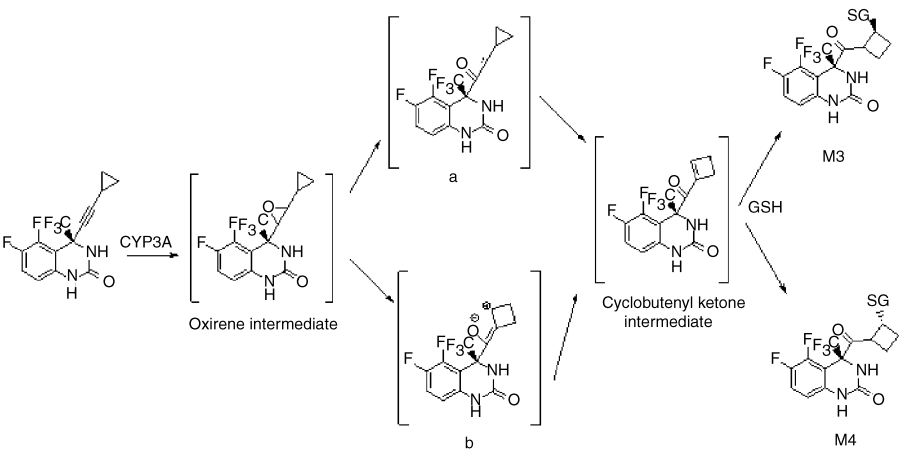

FIGURE 12.13 Proposed metabolic pathways leading to the formation of glutathione adducts in rat.

two methylene proton signals for the cyclopropyl ring (two triplets in 0.2–0.4 ppm range) were missing. Third, the TOCSY experiment indicated a new spin system that involved eight protons and their chemical shift were consistent with a disubstituted cyclobutyl group. These observations pointed toward the cyclopropyl group as the point of modification. Finally, the characteristic ^{1}H NMR signals for the GSH group were also clearly observed and the integration of the GSH hydrogens matched with the rest of the molecule. Based on a combination of NMR evidence, the structures of these two unusual GSH adducts were determined.

In conclusion, NMR is an essential tool for the successful determination of crucial metabolite structures and is routinely used in the pharmaceutical industry. As discussed, metabolite structure problems could be as simple as hydroxylation on an aromatic ring or as complex as a rearrangement depicted in the formation of glutathione adducts. NMR provides a vast and continually expanding combination of techniques applicable to the analysis of metabolite structures. The judicious choice of NMR experiments based on the particulars of the system and the nature of the metabolites can be combined with mass spectrometry and liquid chromatography to successfully analyze a variety of biological metabolites to benefit drug discovery.

REFERENCES

Albert K. Online use of NMR detection in separation chemistry. J Chromatogr A 1995;703:123–147.

Alexander AJ, Xu F, Bernard C. The design of a multidimensional LC–SPE–NMR system (LC2–SPE–NMR) for complex mixture analysis. Magn Reson Chem 2006;44(1):1–6.

Basker MJ, Finch SC, Tyler JW. Use of ^{1}H NMR in the identification of a metabolite of a catecholic cephalosporin excreted in rat bile. J Pharm Biomed Anal 1990;8: 573–576.

Berger S, Braun S. 200 and More NMR Experiments. second ed. John Wiley & Sons; 2004.

Betz M, Saxena K, Schwalbe H. Biomolecular NMR: a chaperone to drug discovery. Curr Opin Chem Biol 2006;10(3):219–225.

Bieri S, Varesio E, Veuthey JL, Muñoz O, Tseng LH, Braumann U, Spraul M, Christen P. Identification of isomeric tropane alkaloids from *Schizanthus grahamii* by HPLC–NMR with loop storage and HPLC–UV–MS/SPE–NMR using a cryogenic flowprobe. Phytochem Anal 2006;17(2):78–86.

Borlak J, Walles M, Elend M, Thum T, Preiss A, Levsen K. Verapamil: identification of novel metabolites in cultures of primary human hepatocytes and human urine by LC–MS(n) and LC–NMR. Xenobiotica 2003;33(6):655–676.

Breitmaier E. Structure Elucidation by NMR in Organic Chemistry: A Practical Guide. Third ed. John Wiley & Sons; 2002.

Bruker Biospin GmbH. Bruker BioSpin announces novel capillary LC–NMR system 2002. Forthcoming.

Buker Biospin GmbH. Bruker BioSpin introduces the CryoFlowProbe, the world's first cryogenic flow-injection NMR probe 2002. Forthcoming, Available at http://www.bruker-biospin.com/nmr/news/pdf_files/cryoflowprb.pdf.

Chando TJ, Everett DW, Kahle AD, Starrett AM, Vachharajani N, Shyu WC, Kripalani KJ, Barbhaiya RH. Biotransformation of irbesartan in man. Drug Metab Dispos 1998;26:408–417.

Chen H, Shockcor J, Chen W, Espina R, Gan LS, Mutlib AE. Delineating novel metabolic pathways of DPC 963, a nonnucleoside reverse transcriptase inhibitor, in rats. Characterization of glutathione conjugates of postulated oxirene and benzoquinone imine intermediates by LC–MS and LC–NMR. Chem Res Toxicol 2002;15:388–399.

Corcoran O, Spraul M. LC–NMR–MS in drug discovery. Drug Discov Today 2003; 8(14):624–631.

Dagnino-Subiabre A, Cassels BK, Baez S, Johansson AS, Mannervik B, Segura-Aguilar J. Glutathione transferase M2-2 catalyzes conjugation of dopamine and dopa *O*-quinones. Biochem Biophys Res Commun 2000;274:32–36.

Daykin CA, VanDuynhoven JPM, Groenewegen A, Dachtler M, Van Amelsvoort JMM, Mulder TPJ. Nuclear magnetic resonance spectroscopic based studies of the metabolism of black tea polyphenols in humans. J Agric Food Chem 2005;53: 1428–1434.

Exarchou V, Godejohann M, van Beek TA, Gerothanassis IP, Vervoort J. LC–UV–solid-phase extraction-NMR–MS combined with a cryogenic flow probe and its application to the identification of compounds present in Greek oregano. Anal Chem 2003;75(22):6288–6294.

Exarchou V, Krucker M, van Beek TA, Vervoort J, Gerothanassis IP, Albert K. LC–NMR coupling technology: recent advancements and applications in natural products analysis. Magn Reson Chem 2005;43(9):681–687.

Freeman R, A Handbook of Nuclear Magnetic Resonance. second ed. Longman Publishing Group; 1997.

Friebolin H, Basic One- and Two-Dimensional NMR Spectroscopy. fourth ed. John Wiley & Sons; 2005.

Froehlich AK, Girreser D, Clement B. Metabolism of *N*-hydroxyguanidines (*N*-hydroxydebrisoquine) in human and porcine hepatocytes: reduction and formation of glucuronides. Drug Metabo Dispos 2005;33:1532–1537.

Gaggelli E, Valensin G. Methods of single- and double-selective excitation: theory and applications. Part II. Conc Magn Reson 1993;5(1):19–42.

Garcia GE, Hicks RP, Skanchy D, Moorad-Doctor DR, Doctor BP, Ved HS. Identification and characterization of the major huperzine a metabolite in rat blood. J Anal Toxicol 2004;28:379–383.

Gerhard U, Thomas S, Mortishire-Smith R. Accelerated metabolite identification by "extraction-NMR". J Pharm Biomed Anal 2003;32:531–538.

Godejohann M, Tseng LH, Braumann U, Fuchser J, Spraul M. Characterization of a paracetamol metabolite using on-line LC–SPE–NMR–MS and a cryogenic NMR probe. J Chromatogr A 2004;1058(1–2):191–196.

Hajduk PJ. SAR by NMR: putting the pieces together. Mol Interv 2006;6(5):266–272.

Homans SW. A Dictionary of Concepts in NMR. Second ed. Oxford University Press; 2005.

Hwang TL, Shaka AJ. Water suppression that works. Excitation sculpting using arbitrary wave-forms and pulsed-field gradients. J Magn Reson Series A 1995; 112(2):275–279.

Iwasa K, Kuribayashi A, Sugiura M, Moriyasu M, Lee DU, Wiegrebe W. LC–NMR and LC–MS analysis of 2,3,10,11-oxygenated protoberberine metabolites in Corydalis cell cultures. Phytochemistry 2003;64(7):1229–1238.

Jairaj M, Watson DG, Grant MH, Gray AI, Skellern GG. Comparative biotransformation of morphine, codeine and pholcodine in rat hepatocytes: identification of a novel metabolite of pholcodine. Xenobiotica 2002;32:1093–1107.

Keeler J. Understanding NMR Spectroscopy. first ed. UK: John Wiley and Sons; 2005.

Keun HC, Beckonert O, Griffin JL, Richter C, Moskau D, Lindon JC, Nicholson JK. Cryogenic probe ^{13}C NMR spectroscopy of urine for metabonomic studies. Anal Chem 2002;74:4588–4593.

Klaus A. On-line LC–NMR and Related Techniques, first ed. E-Book;2003.

Kupee E. NMR at 900 MHz. Chem Heter Comp 2001;37(11):1429–1438.

Lepre CA, Moore JM, Peng JW. Theory and applications of NMR-based screening in pharmaceutical research. Chem Rev 2004:104(8):3641–76

Lindon JC, Nicholson JK, Wilson ID. The development and application of coupled HPLC–NMR spectroscopy. Adv Chromatogr 1996;36:315–382.

Lyčka A, Fryšová I, Slouka J. An anomalous course of the reduction of 2-(3-oxo-3,4-dihydroquinoxalin-2-yl)benzene diazonium salt: a reinvestigation. Magn Reson Chem 2007;45(1):46–50.

Martin G, Zektzer A, Two-Dimensional NMR Methods for Establishing Molecular Connectivity. First ed. VCH; New York: 1998.

Moreno A, Daz-Ortiz A, Dez-Barra E, de la Hoz A, Langa F, Prieto P, Claridge TDW. Determination of the stereochemistry of four spirodiastereoisomers by one- and two-dimensional NOE studies. Magn Reson Chem 1996;34(1):52–58.

Munro SLA, Craik DJ. NMR conformational studies of fenamate non-steroidal antiinflammatory drugs. Magn Reson Chem 1994;32(6):335–342.

NMR probes. Varian Inc, Palo Alto, CA, USA;2002. Available at http://www.varianinc.com/cgi-bin/nav?varinc/docs/nmr/products/probes.

Orry AJ, Abagyan RA, Cavasotto CN. Structure-based development of target-specific compound libraries. Drug Discov Today 2006;11(5–6):261–266.

Pellecchia M. Solution nuclear magnetic resonance spectroscopy techniques for probing intermolecular interactions. Chem Biol 2005;12(9):961–971.

Reilly CA, Ehlhardt WJ, Jackson DA, Kulanthaivel P, Mutlib AE, Espina RJ, Moody DE, Crouch DJ, Yost GS. Metabolism of capsaicin by cytochrome P450 produces novel dehydrogenated metabolites and decreases cytotoxicity to lung and liver cells. Chem Res Toxicol 2003;16(3):336–349.

Schaefer M, Faller P, Nicole D. Regio- and stereoselective alkylation of a pyrrolidinic system: structural and conformational studies by high field NMR techniques. Org Magn Reson 1982;19(2):108–111.

Schlotterbeck G, Ross A, Hochstrasser R, Senn H, Kuhn T, Marek D, Schett O. High-resolution capillary tube NMR. A miniaturized 5 mL high-sensitivity TXI probe for mass-limited samples, off-line LC NMR, and HT NMR. Anal Chem 2002;74: 4464–4471.

Schutz A, Golbik R, Konig S, Hubner G, Tittmann K. Intermediates and transition states in thiamin diphosphate-dependent decarboxylases. A kinetic and NMR study on wild-type indolepyruvate decarboxylase and variants using indolepyruvate, benzoylformate, and pyruvate as substrates. Biochemistry 2005;26:44916):6164–79.

Seger C, Godejohann M, Spraul M, Stuppner H, Hadacek F. Reaction product analysis by high-performance liquid chromatography-solid-phase extraction-nuclear magnetic resonance Application to the absolute configuration determination of naturally occurring polyyne alcohols. J Chromatogr A 2006;1136(1):82–88.

Sem DS, Pellecchia M. NMR in the acceleration of drug discovery. Curr Opin Drug Discov Devel 2001;4(4):479–492.

Shockcor PJ, Unger SH, Wilson ID, Foxall PJD, Nicholson JK, Lindon JC. Combined hyphenation of HPLC, NMR spectroscopy and ion trap mass spectrometry (LC–NMR–MS) with application to the detection and characterization of xenobiotic and endogenous metabolites in human urine. Anal Chem 1996;68:4431–4435.

Smallcombe SH, Patt SL. WET solvent suppression and its applications to LC–NMR and high-resolution NMR spectroscopy. J Magn Reson Series A 1995;117(2):295–303.

Spraul M, Hofmann M, Lindon JC, Farrant RD, Seddon MJ, Nicholson JK, Wilson ID. Evaluation of liquid-chromatography coupled with high-field ^{1}H NMR spectroscopy for drug metabolite detection and characterization: the identification of paracetamol metabolites in urine and bile. NMR Biomed 1994;7:295–303.

Spraul M, Hofmann M, Dvortsak P, Nicholson JK, Wilson ID. High-performance liquid chromatography coupled to high-field proton nuclear magnetic resonance spectroscopy: application to the urinary metabolites of ibuprofen. Anal Chem 1993;65:327–330.

Spraul M, Freund AS, Nast RE, Withers RS, Maas WE, Corcoran O. Advancing NMR sensitivity for LC–NMR–MS using a cryoflow probe: application to the analysis of acetaminophen metabolites in urine. Anal Chem 2003;75(6):1536–1541.

Sridharan V, Saravanan S, Muthusubramanian S, Sivasubramanian S. NMR investigation of hydrogen bonding and 1,3-tautomerism in 2-(2-hydroxy-5-substituted-aryl) benzimidazoles. Magn Reson Chem 2005;43(7):551–556.

Valente AP, Miyamoto CA, Almeida FC. Implications of protein conformational diversity for binding and development of new biological active compounds. Curr Med Chem 2006;13(30):3697–3703.

Wilson SR, Malerd H, Petersen D, Simic N, Bobu MM, Rise F, Lundanes E, Greibrokk T. Controlling LC–SPE–NMR systems. J Sep Sci 2006;29(4):582–589.

Xu F, Alexander AJ. The design of an on-line semipreparative LC–SPE–NMR system for trace analysis. Magn Reson Chem 2005;43(9):776–782.

Yang Z. Online hyphenated liquid chromatography–nuclear magnetic resonance spectroscopy–mass spectrometry for drug metabolite and nature product analysis. J Pharm Biomed Anal 2006;40(3):516–527.

Zartler ER, Shapiro MJ. Protein NMR-based screening in drug discovery. Curr Pharm Des 2006;12(31):3963–3972.

Zhang D, Zhao W, Roongta VR, Mitroka JG, Klunk LJ, Zhu M. Amide N-glucuronidation of MaxiPost catalyzed by UDP-glucuronosyltransferase 2B7 in humans. Drug Metab Dispos 2004;32:545–551.

Zhou CC, Hill DR. The keto–enol tautomerization of ethyl butylryl acetate studied by LC–NMR. Magn Reson Chem 2006;45(2):128–132.